

MONOTROPA HYPOPITYS MEDIATED METAL (Ag, Ni AND Cu) NANOPARTICLES IN MICROBIAL INHIBITION AND MERCURY (II) ION DETECTION

NARGIS JAMILA^{1*}, NAEEM KHAN², KOUSAR KHAN¹, NADIA BIBI³, FAHEEM ULLAH⁴,
AALIYA MINHAZ¹, FATIMA JAVED¹, SANA IHSAN¹ AND HAFIZA SALMA BIBI¹

¹Department of Chemistry, Shaheed Benazir Bhutto Women University, Peshawar 25000, Khyber Pakhtunkhwa, Pakistan

²Department of Chemistry, Kohat University of Science and Technology, Kohat 26000, Khyber

³Department of Microbiology, Shaheed Benazir Bhutto Women University, Peshawar 25000, Khyber Pakhtunkhwa, Pakistan

⁴Department of Chemistry, Abdul Wali Khan University Mardan, Mardan, Khyber Pakhtunkhwa, Pakistan

*Corresponding author's email: njk985@gmail.com, nargisjamila@sbbwu.edu.pk

Abstract

Green synthesis utilizing plants, algae, fungi and microorganisms for nanoparticles have been drawing attention due to environmental friendly, rapid, and profitable properties. This study was designed to synthesize silver, nickel and copper nanoparticles using a saprophytic plant; *Monotropa hypopitys* aqueous extract. In addition, the application as antioxidant, antimicrobial, and detection of mercury (II) in tap water were also evaluated. Well-defined and stable nanoparticles (NPs) were formed in 1:9 (copper NPs), 1:10 (nickel NPs), and 1:14 (silver NPs) ratios. Furthermore, *M. hypopitys* mediated nanoparticles (MHNPs) exhibited significant antioxidant, antimicrobial, and heavy metal sensing properties. This study concluded the promising pharmacological and environmental remediation application of the synthesized MHNPs.

Key words: *M. hypopitys*, Nanoparticles, Antimicrobial, Mercury (II), tap water

Introduction

Nanoparticles (NPs); cluster of atoms in a size of 1–100 nm, perform unique properties and potential application in catalysis, electronic and medical devices, sensing, and drug delivery. The physical and chemical methods of coprecipitation, sol-gel, microemulsion, and laser ablation might produce well-defined NPs but with less effective pharmacological properties, and are toxic to environment (Ali *et al.*, 2016; Raghunath, & Perumal, 2017; Khan *et al.*, 2019; Nithya & Sundrarajan, 2020). Hence, it is essential to explore environmental friendly and green methods using bacteria, fungi, algae, yeast, and plants, which are a rich source of molecules acting as reducing as well as stabilizing agents for NPs synthesis (Singh *et al.*, 2016; Ahmed *et al.*, 2017; Saratale *et al.*, 2018; Puja & Kumar, 2019). Biological synthesis is an environmental friendly, simple, efficient, cost effective, which are making them effective drugs carrier in drug design, delivery, and development (Ayodhya & Veerabhadram, 2017; Mirzaei & Darroudi, 2017; Das *et al.*, 2018).

Silver nanoparticles (AgNPs) have great importance due to their wide range of applications in catalysis, environmental pollutants removal, cancer therapy, and

antimicrobial properties (Dinda *et al.*, 2019; Samuel *et al.*, 2020; Jamila *et al.*, 2020a; Jamila *et al.*, 2020b). Similarly, nickel and copper NPs play key role in biomedicines as antimicrobial, anti-inflammatory, and anticancer agents (Din *et al.*, 2018; Agarwal *et al.*, 2019; Ahmed *et al.*, 2019; Wu & Kong, 2020). In the current study, mediated silver, nickel, and copper oxide NPs were synthesized utilizing *Monotropa hypopitys* (*M. hypopitys*) aqueous extract.

M. hypopitys (pinesap) is a non-photosynthetic and achlorophyllous plant (Fig. 1) belonging to family Ericaceae or Pyrolaceae (Beletsky *et al.*, 2017). The greater part of the year, it exists as a stretched underground rhizome, on which *chlorophyll* generative shoots made out of leaves (bracts), and inflorescences are framed toward the start of July. As *M. hypopitys* is achlorophyllous, therefore, it absorbs nutrients through the fungi connected to its roots close-by trees (Beletsky *et al.*, 2017). Locally, this saprophytic plant is specifically used for the treatment of whooping cough. Very few and old literature on its phytochemical investigation is available reporting the isolation of glucoside, furochroman, chloromycorrhizin A and mycorrhizin A from its roots (Trim, 1951, Trofast, 1978).



Fig. 1. *M. hypopitys* whole plant.

To the best, the author found that there is no any previous research work related to *M. hypopitys* mediated nanoparticles and the evaluation as biological and environmental remediation agent. Considering the novelty of the *M. hypopitys*, and the importance of NPs, this study was designed to synthesize silver (MHAgnPs), nickel (MHNiNPs), and copper oxide nanoparticles (MHCuONPs) using aqueous extract of *M. hypopitys*. The synthesized NPs were characterized by ultra violet-visible (UV-Vis), Fourier transform-infrared (FT-IR), and scanning electron microscopy (SEM) techniques. As nanoparticles have been proven the promising pharmacological agents (Chen *et al.*, 2016; Hossainzadeh *et al.*, 2019), therefore, the subject synthesized NPs were examined for antioxidant, and antimicrobial properties.

In this modern era, due to increased technology, industrialization, fuels, and anthropogenic activities, the toxic metals such as arsenic (As), cadmium (Cd), mercury (Hg), and lead (Pb) are contaminating the living system and lethal to them even at very low concentration. Among these metals, mercury (Hg) is a hazardous pollutant and bioaccumulative neurotoxin emitted into the atmosphere through natural as well as anthropogenic activities causing lethal health damages to the living organisms. Therefore, to ensure the environment safety, it is crucial to design the robust and efficient methods to monitor, quantify, and remove these toxic metals from the environment including water, soil, and plants. Metal nanoparticles (MNPs), due to the increased surface area and well-dispersed size have been widely used in the colorimetric and chemical sensing of these toxic metal ions (Priyadarshini & Pradhan, 2017). In this research work, a facile and sensitive method of using MHNPs for chromogenic detection of Hg (II) in real tap water sample of Peshawar was used. This is the first report, which describes the synthesis of silver, nickel and copper nanoparticles using *M. hypopitys*, and the application as antioxidant, antimicrobial and heavy metal sensing properties.

Materials and Methods

Sample collection: The whole plant; *M. hypopitys* was collected from Zarki Nasratti (Marrisaam), District Karak, Khyber Pakhtunkhwa, Pakistan. Before use, the subject sample was cleaned to remove all the dust, and then dried and stored the sample for further use. The collected plant was cut into small pieces and grinded into powder. Then, 25 g sample was taken and dissolved in distilled water stirred for 1 hour on 500 rpm at 40 degrees temperature. The *M. hypopitys* aqueous extract (MHAE) was filtered and used for further analysis.

Chemicals and instrumentation: Chemicals for nanoparticles synthesis; silver nitrate (AgNO_3), $\text{CuSO}_4 \cdot 5\text{H}_2\text{O}$, and NiCl_2 , antioxidant activity; 2,2-diphenyl-1-picrylhydrazyl (DPPH), gallic acid, and trolox, and microbial strains; *Staphylococcus aureus*, *Bacillus subtilis*, *Pseudomonas aeruginosa*, *Escherichia coli*, *Candida albicans*, *Candida krusei*, *Aspergillus flavus*, and *Trichophyton mentagrophytes*, nutrient agar (Muller Hinton Broth), *p*-iodonitrotetrazolium chloride (INT), vancomycin, streptomycin, fluconazole, and

amphotericin were purchased from Sigma, Merck and Oxoid companies. The synthesized MHNPs were characterized by UV-vis spectrophotometer (UV-1800, Shimadzu, Japan) for optical properties. The infrared spectra ($400\text{--}4000\text{ cm}^{-1}$) were recorded by Fourier-transform infrared spectrometer (Bruker). Scanning electron microscope (JSM-5910) was used for size and shape determination.

Synthesis of MHNPs: MHNPs were synthesized by utilizing *M. hypopitys* aqueous extract and salts including silver nitrate, nickel chloride, and copper sulfate solutions using different ratios and conditions; incubation, stirring, heating, and sunlight. The schematic synthesis is illustrated in (Fig. 2.) UV-vis spectra of all the mixtures were recorded at 30 min to 300 min. After that, MHNPs were collected from the whole solution by centrifugation at 4000 rpm x g. The final product was dried in oven min and stored in airtight vial for further analysis.

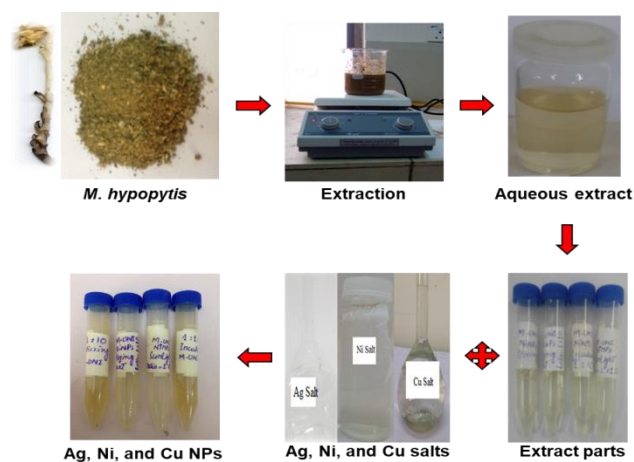


Fig. 2. Procedure of *M. hypopitys* mediated Ag, Ni, and Cu nanoparticles synthesis.

Antioxidant and antimicrobial activities of MHNPs:

The antioxidant activity of MHNPs was evaluated using an established 2,2-diphenyl-1-picrylhydrazyl (DPPH) assay (Jamila *et al.*, 2014). Briefly, each sample (150 μL) was mixed with DPPH solution (2850 μL), and incubated overnight in the dark. After 24 h, the absorbance of the mixture was measured at 515 nm. A blank, a negative control, and the standards (gallic acid, trolox) were also analyzed. The inhibition percentage of DPPH radical by MHAE and MHNPs was calculated according to the given formula:

$$\% \text{ Inhibition} = [(1 - (A_{\text{sample}}/A_{\text{control}}))] \times 100$$

The results of radical scavenging ability of MHNPs were expressed as IC_{50} calculated in Graphpad Prism 7. Antimicrobial activities were evaluated using Muller-Hinton agar (MHA) and broth (MHB) micro-dilution methods. The bacterial strains were *Bacillus subtilis* and *Staphylococcus aureus* (Gram-positive), and *Escherichia coli* and *Pseudomonas aeruginosa* (Gram-negative). Four yeasts; *Candida albicans*, *Candida krusei*, *Aspergillus flavus*, and *Trichophyton mentagrophyte* were also used. The glassware were decontaminated using aqua regia

(HCl/HNO₃) and deionized water. In Disc diffusion assay, an inoculum (100 µL) was streaked on the Mueller–Hinton agar surface using a sterile cotton swap. Then, sterile paper disc impregnated with 20 µL MHNPs (2 mg/mL), and the standard drugs (streptomycin, vancomycin) were kept on the inoculated agar. They were then incubated (37°C) for 24 h. The diameters of inhibition zone were then measured in millimeters (mm). Besides, broth microdilution assay or minimal inhibitory concentration (MIC) method using sterile flat-bottom 96-well plates was performed.

MHNPs for detection of mercury (II) in tap water: The practical application of the synthesized MHNPs was determined for mercury (II) ions recognition in the samples of routine tap water collected from Peshawar city. The spiking of the samples was carried out with Hg (II) ions solution (0.1 mM).

Results and Discussion

Synthesis and characterization of MHNPs: This study reports the green synthesis of AgNPs, CuONPs, and NiNPs using *M. hypopitys* aqueous extract. In NPs synthesis, Ag⁺, Cu⁺⁺, Ni⁺⁺ oxidize the O-H group of phytochemicals present in the extract to C=O group and itself reduce to metallic Ag⁰, Cu⁰, Ni⁰. NPs show surface Plasmon resonance (SPR) and absorption band due to the coherent oscillation metal electrons. The shape, width, and position of SPR band depend on the NPS size and distribution. A red shift of SPR occurs as the size of NPs

increases, and vice versa. For monodispersed size distribution NPs, the shape of SPR peak is symmetrical, which broadens upon non-uniform size distribution (Jana *et al.*, 2016). In this study, MHNPs were synthesized in 1:1 to 1:15 ratio under the conditions of stirring, heating, incubation, and sunlight. The subject synthesized MHNPs were then characterized by the fundamental UV-vis spectroscopic technique.

For MHAgnPs, the absorption peak appeared at 400-440 nm whereas for MHNiNPs and MHCuONPs, the SPR exhibited at 250-350 nm (Peng *et al.*, 2017). Synthesizing AgNPs, the ratios 1:9 and 1:10 resulted in AgNPs formation exhibiting an absorption peak at 425 nm (Fig. 3). In 1:9 ratio, under heating (50°C) and stirring (500 rpm), the significant and monodispersed NPs were formed (Figure 3a). However, using this ratio, the other conditions did not result in NPs. Utilizing 1:10 ratio, all the 4 conditions, yielded AgNPs, with the most significant under stirring (Fig. 3b-e). Furthermore, when the AgNPs synthesis were tried using 1:13 ratio, it was found that all of the conditions resulted in unstable AgNPs formation (Fig. 4). Concerning the MHNiNPs and MHCuONPs synthesis, the formation was preliminary indicated by color change of the reaction mixture (1:10 for NiNPs, and 1:9 for CuONPs) from dark green to light green, and blue to colourless, respectively. The conditions of stirring and heating, stirring and sunlight have significant role in the formation of NiNPs (Fig. 5). Regarding the MHCuONPs, also heating and stirring in a 1:9 ratio yielded significant NPs, which exhibited a peak at around 337 nm (Fig. 6).

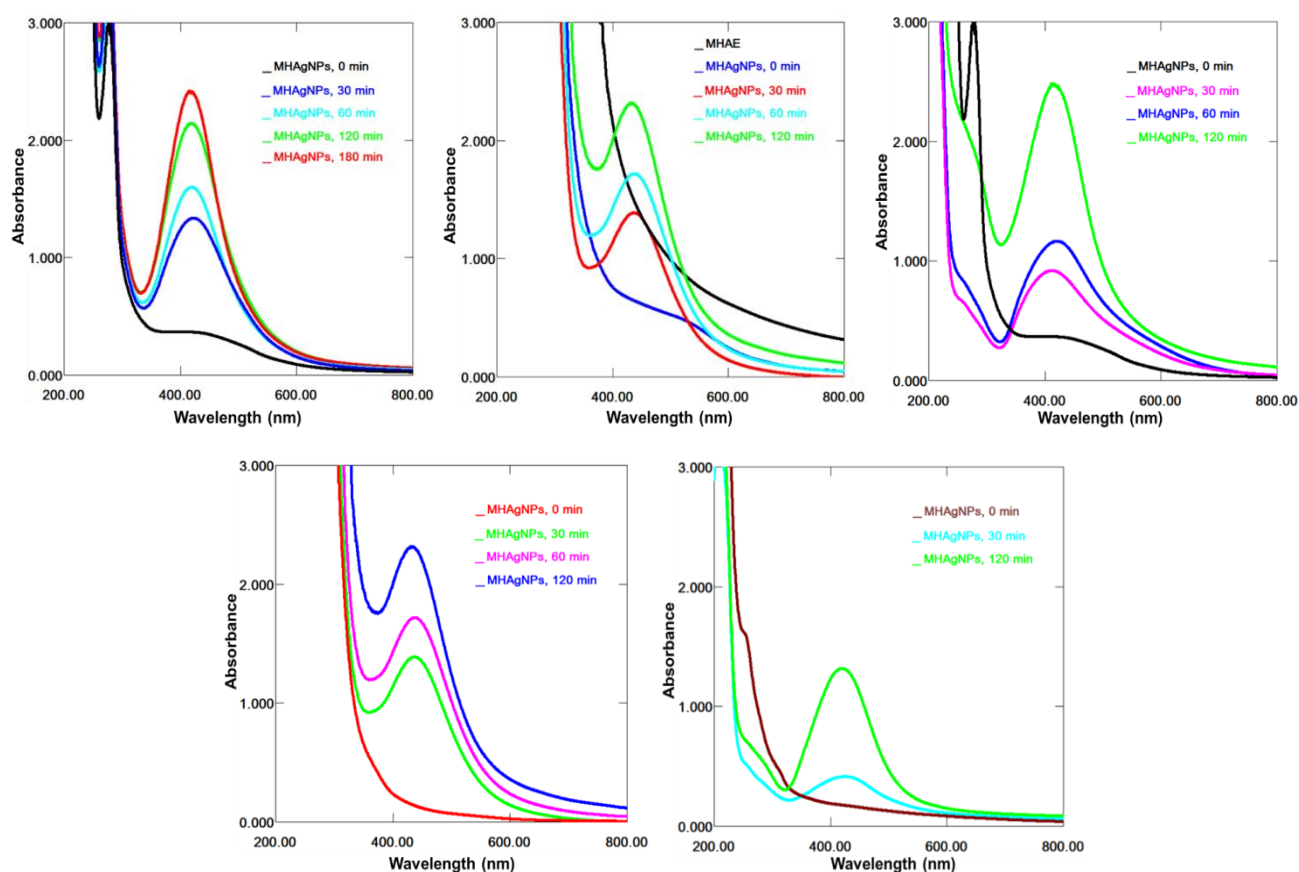


Fig. 3. UV spectra (200-800 nm) of MHAgnPs synthesized in (a) 1:9 heating and stirring, (b) 1:10 heating and stirring, (c) 1:10 sunlight, (d) 1:10 stirring, and (e) 1:10 incubation.

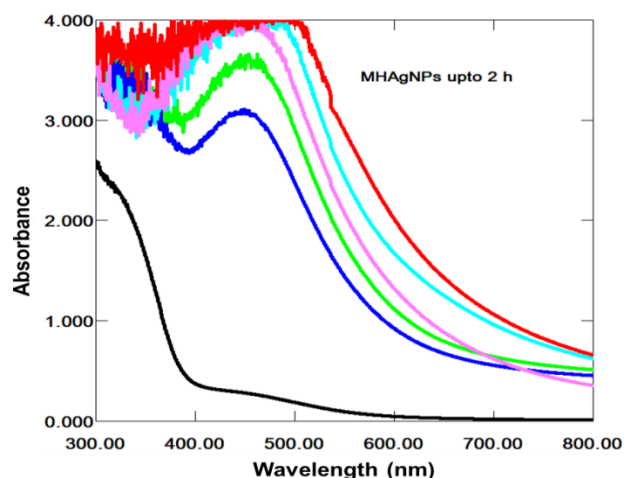


Fig. 4. No stable MHAgNPs formed in 1: 13 ratio under stirring, heating +stirring, sunlight, and incubation.

Phytoconstituents including phenolics, flavonoids, and alkaloids due to $-OH$ group have potential of reducing metal ions (M^+/M^{++}) into zero-valent states (M^0). In microbial NP synthesis, the reductase enzyme of microbial cell wall reduces the metal ions into elemental

metal (Johnson & Uwa, 2019). FT-IR spectra (Fig. 7) showed that OH group in the phytochemicals of *M. hypopitys* aqueous extract reduced the metal salts into their respective NPs. A major peak at $3500-3200\text{ cm}^{-1}$ ($O-H$) reduced in intensity, which might be considered to involve in the formation of NPs. Furthermore, SEM images (Fig. 8) indicated the AgNPs having size of 57 nm whereas NiNPs and CuONPs were triangular in shape having sizes of 79 and 83 nm, respectively.

Antioxidant and antimicrobial activities of MHNPs:

The antioxidant potential of MHNPs was examined by DPPH radical scavenging assay in which the violet DPPH radical solution changes to yellow solution of reduced DPPH by phenolics. The results of antioxidant activity of *M. hypopitys* mediated NPs (Fig. 9) showed that MHNiNPs is the most active antioxidant agent against DPPH with IC_{50} value of 1.52 mg/mL, as compared to MHCuONPs ($IC_{50} = 1.80\text{ mg/mL}$) and MHAgNPs ($IC_{50} = 2.19\text{ mg/mL}$). The nonlinear graph of DPPH inhibition was found to be dose-dependent increasing with increased samples concentration.

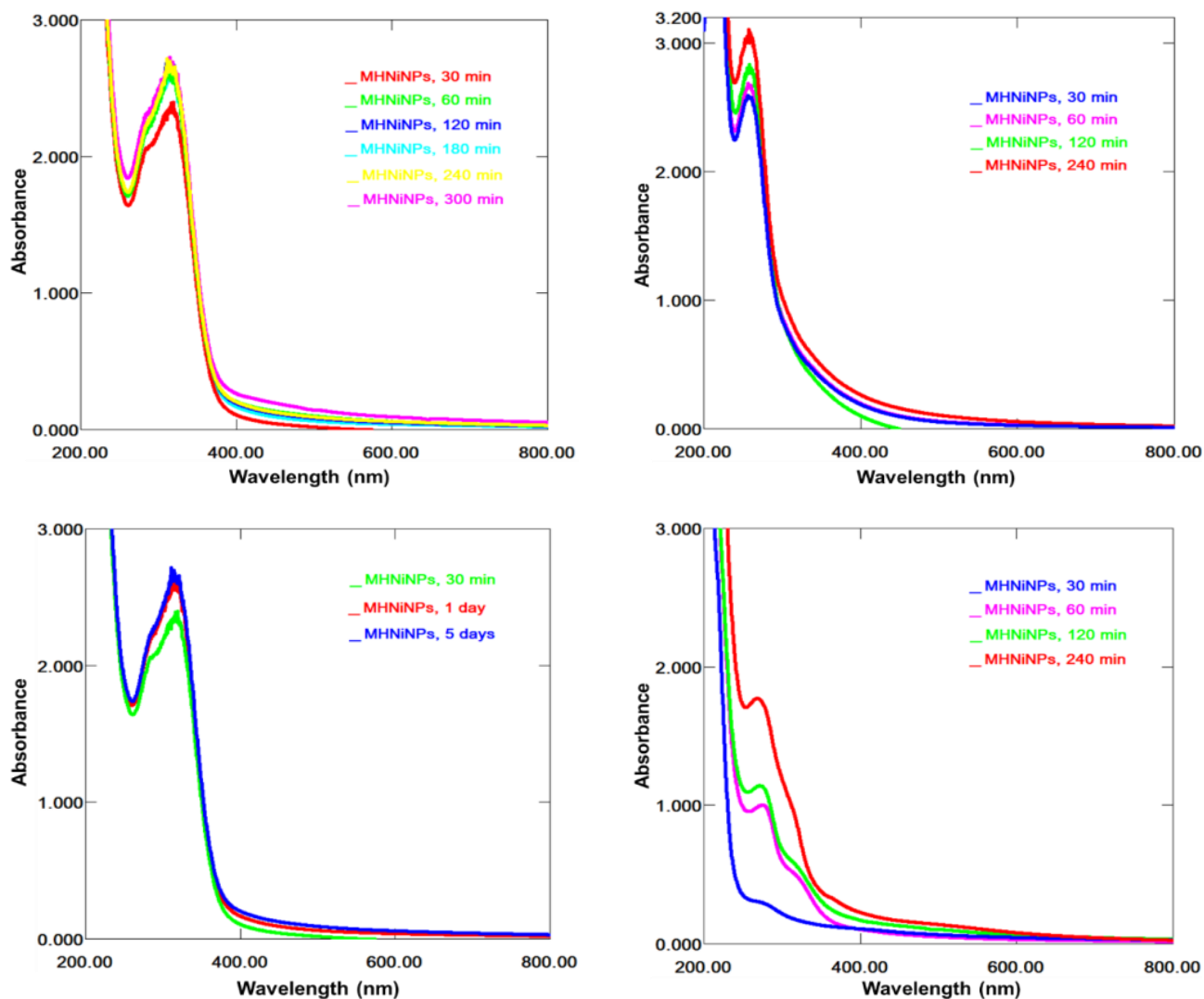


Fig. 5. UV spectra (200-800 nm) of MHNiNPs synthesized in 1:10 ratio (a) heating and stirring (b) stirring, (c) sunlight, and (d) incubation.

Table 1. Antibacterial activity by disc diffusion (DD, mm) and minimum inhibitory concentration (MIC, µg/mL) methods of MHAE, MHAgNPs, MHCuONPs, and MHNiNPs.

Samples	Disk diffusion (mm)				Minimum inhibitory concentration method (µg/mL)			
	<i>S. aureus</i>	<i>B. subtilis</i>	<i>P. aeruginosa</i>	<i>E. coli</i>	<i>S. aureus</i>	<i>B. subtilis</i>	<i>P. aeruginosa</i>	<i>E. coli</i>
MHAE	10.0	10.0	6.0	6.0	1000	1000	1000	1000
MHAgNPs	20.0	21.0	15.0	15.0	62.5	62.5	125.0	125.0
MHCuONPs	16.0	18.0	14.0	14.0	125.0	125.0	250.0	250.0
MHNiNPs	16.0	14.0	13.0	12.0	125.0	125.0	250.0	250.0
Vancomycin*	19.0	21.0	11.0	12.0	31.25	31.25	250.0	250.0
Streptomycin*	19.0	23.0	15.0	19.0	31.25	31.25	250.0	250.0

Antifungal activity

Samples	Disk diffusion (mm)				Minimum inhibitory concentration method (µg/mL)			
	<i>C. albicans</i>	<i>C. krusei</i>	<i>A. flavus</i>	<i>T. mentagrophytes</i>	<i>C. albicans</i>	<i>C. krusei</i>	<i>A. flavus</i>	<i>T. mentagrophyte</i>
MHAE	8.0	6.0	7.0	7.0	1000	1000	1000	1000
MHAgNPs	19.0	18.0	16.0	17.0	62.5	125.0	125.0	125.0
MHCuONPs	16.0	15.0	16.0	13.0	250.0	250.0	250.0	250.0
MHNiNPs	16.0	16.0	14.0	15.0	62.5	250.0	250.0	250.0
Fluconazole*	19.0	21.0	25.0	25.0	31.25	31.25	62.5	125.0
Amphotericin*	17.0	18.0	25.0	24.0	250.0	250.0	250.0	250.0

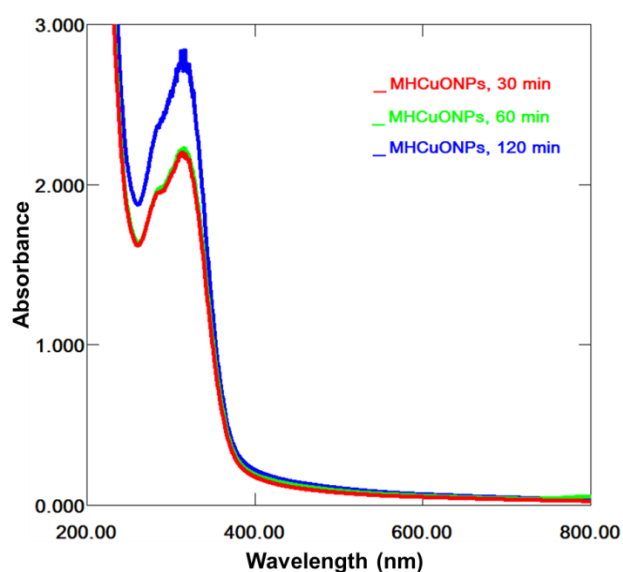


Fig. 6. UV spectra (200-800 nm) of MHCuONPs synthesized in 1:9 ratio under heating and stirring.

In antimicrobial activity, the inhibition zones (15-21 mm) and MIC values (62.5 to 125.0 µg/mL) in case of MHAgNPs against bacterial strains confirmed that these NPs have high antibacterial activity as compared to that of MHNiNPs and MHCuONPs (12-18 mm and 125.0 to 250.0 µg/mL, respectively). The NPs were the most effective against Gram-positive strains as compared to Gram-negative with the least inhibitory effect against *P. aeruginosa* and *E. coli* as indicated by their zone of inhibition and MIC values (Table 1). In antifungal activity, MHAgNPs have shown the highest inhibition (19.0 mm) and the least MIC value (62.5 µg/mL) against *C. albicans* (Table 1) indicating the significant activity compared to standard, amphotericin (17.0 mm and 250.0 µg/mL). The other NPs were comparatively less active.

The significant inhibition by the subject NPs against different microbes could be due to their increased surface area enhancing its exposure to receptor sites.

Detection of mercury (II) ions via MHNPs in tap water samples:

The chemosensing potential of MHNPs was examined by mixing different 0.1 mM metal salts; cobalt (I), Copper (I), sodium (I), potassium (I), iron (II), iron (III), and mercury (II) solutions in 1:1 ratio with MHNPs. From the reaction, only the color disappearance of MHNPs with mercury (II) ions was observed, which indicated the detection of mercury (II) ions with naked eye. Hence, the subject MHNPs were used for mercury (II) ions sensing in tap water samples. The results (Fig. 10) of the spiked samples indicated that an SPR bands of MHNPs significantly decreased in the sample of tap water. Hence, this sensing probe could significantly use to detect mercury (II) in water and other biological samples required for medical diagnosis.

Conclusions

This study provides green synthesis of Ag, Ni, and Cu nanoparticles by using saprophytic plant; *M. hypopitys* aqueous extract. From the results of the antioxidant, antimicrobial, and heavy metal sensing evaluation of the synthesized MHNPs, it was concluded that these NPs could be beneficial in the fields of environmental remediation and nanomedicine. The biological and clinical applications of the subject NPs are currently under investigation.

Acknowledgements

This research study was supported by the research grant; 8967/KPK/NRPU/R&D/HEC/2017. The authors are thankful to the Higher Education Commission (HEC) for awarding this project.

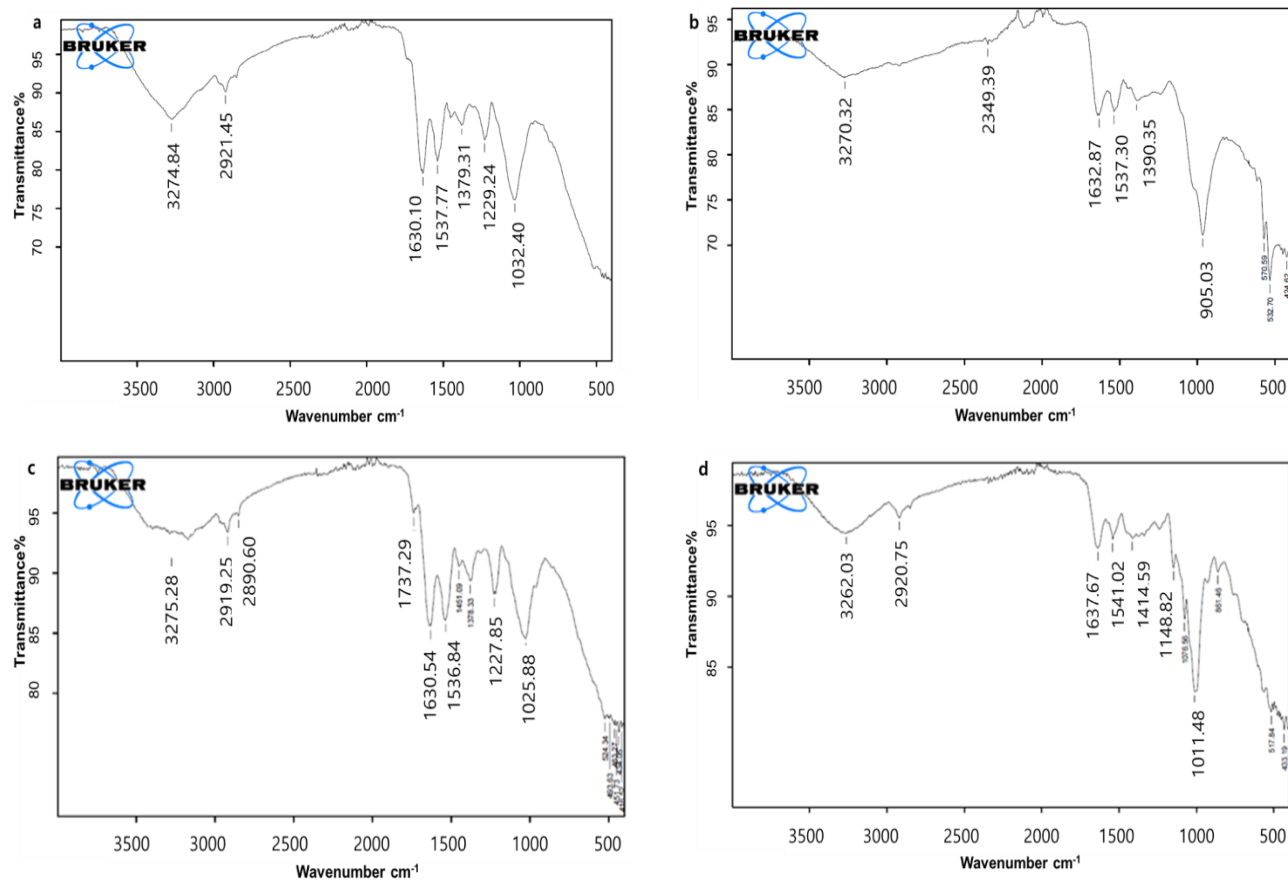


Fig. 7. IR spectra ($4000\text{--}400\text{ cm}^{-1}$) of (a) *M. hypopitys* aqueous extract (MHAE), (b) MHAgNPs, (c) MHNiNPs, and (d) MHCuONPs.

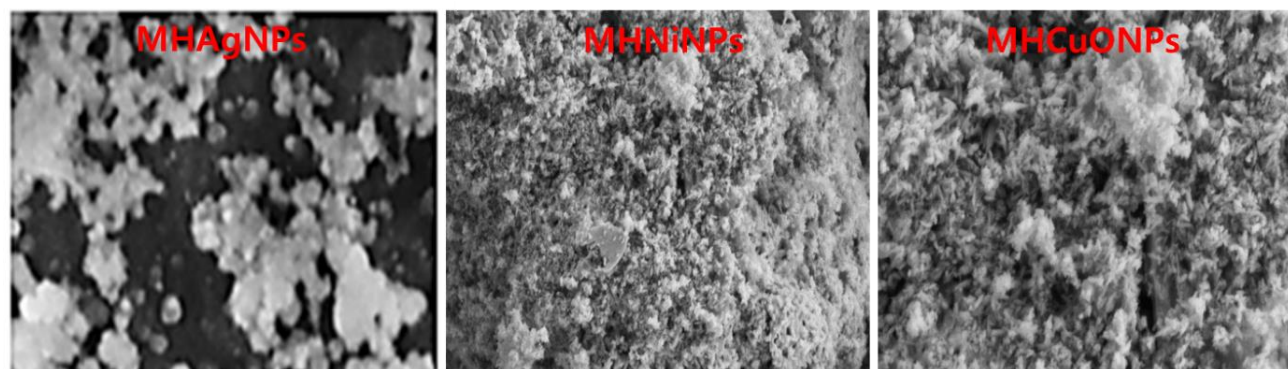


Fig. 8. SEM images of MHAgNPs, MHNiNPs, and (c) MHCuONPs.

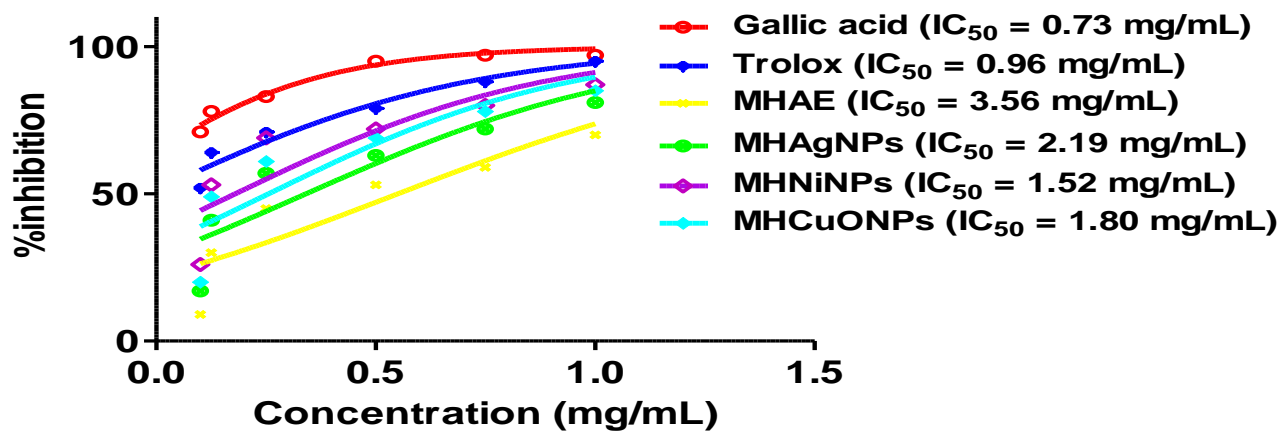


Fig. 9. DPPH radical inhibition activity of (a) MHAE and MHNPs.

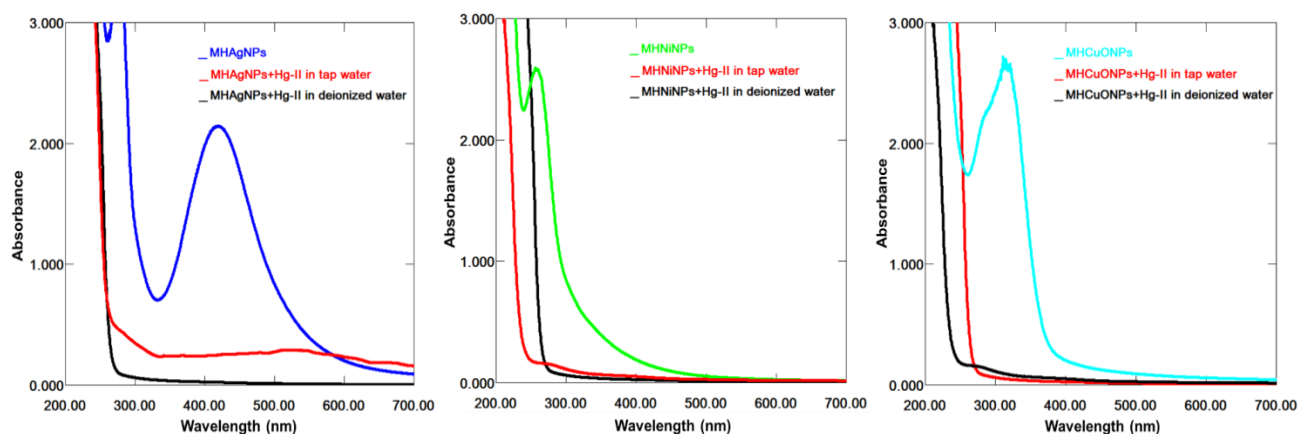


Fig. 10. UV-vis spectra of (a) MHAgnPs, (b) MHNiNPs, and (c) MHCuONPs detection system of mercury (II) in tap water samples.

References

- Agarwal, H., A. Nakara and V.K. Shanmugam. 2019. Anti-inflammatory mechanism of various metal and metal oxide nanoparticles synthesized using plant extracts: A review. *Biomed. Pharm.*, 109: 2561-2572.
- Ahmed, S., S.A. Chaudhry and S. Ikram. 2017. A review on biogenic synthesis of ZnO nanoparticles using plant extracts and microbes: a prospect towards green chemistry. *J. Photochem. Photobiol.*, 166: 272-284.
- Ahmed, A., M. Usman, Q.Y. Liu, Y.Q. Shen, B. Yu and H.L. Cong. 2019. Plant mediated synthesis of copper nanoparticles by using *Camelia sinensis* leaves extract and their applications in dye degradation. *Ferroelectrics*, 549(1): 61-69.
- Ali, A., Z. Hira, M. Zia, I. ul Haq, A.R. Phull, J.S. Ali and A. Hussain. 2016. Synthesis, characterization, applications, and challenges of iron oxide nanoparticles. *Nanotechnol. Sci. Appl.*, 9: 49-67.
- Ayodhya, D. and G. Veerabhadram. 2017. One-pot green synthesis, characterization, photocatalytic, sensing and antimicrobial studies of *Calotropis gigantea* leaf extract capped CdS NPs. *Mat. Sci. Eng.*, 225: 33-44.
- Beletsky, A.V., M.A. Filyushin, E.V. Gruzdev, A.M. Mazur, E.B. Prokhortchouk, E.Z. Kochieva, A.V. Mardanov, N.V. Ravin and K.G. Skryabin. 2017. De novo transcriptome assembly of the mycoheterotrophic plant *Monotropa hypopitys*. *Genom. Data*, 11: 60-61.
- Chen, J., Z. Guo, H. Tian and X. Chen. 2016. Production and clinical development of nanoparticles for gene delivery. *Mol. Ther. Methods Clin. Dev.*, 3: 16023.
- Das, P., S. Ghosh, R. Ghosh, S. Dam and M. Baskey. 2018. *Madhuca longifolia* plant mediated green synthesis of cupric oxide nanoparticles: A promising environmentally sustainable material for waste water treatment and efficient antibacterial agent. *J. Photochem. Photobiol.*, 189: 66-73.
- Din, M.I., A.G. Nabi, A. Rani, A. Aihetasham and M. Mukhtar. 2018. Single step green synthesis of stable nickel and nickel oxide nanoparticles from *Calotropis gigantea*: catalytic and antimicrobial potentials. *Environ. Nanotechnol. Monit. Manag.*, 9: 29-36.
- Dinda, G., D. Halder, A. Mitra, N. Pal and D.K. Chattoraj. 2019. Phytosynthesis of silver nanoparticles using *Zingiber officinale* extract: evaluation of their catalytic and antibacterial activities. *J. Disper. Sci. Technol.*, 1-8.
- Hossainzadeh, S., N. Ranji, A.N. Sohi and F. Najafi. 2019. Silibinin encapsulation in polymersome: A promising anticancer nanoparticle for inducing apoptosis and decreasing the expression level of miR-125b/miR-182 in human breast cancer cells. *J. Cell. Physiol.*, 234: 22285-22298.
- Jamila, N., M. Khairuddean, S.N. Khan and N. Khan. 2014. Complete NMR assignments of bioactive rotameric (3→8) biflavonoids from the bark of *Garcinia hombroniana*. *Magn. Reson. Chem.*, 52: 345-352.
- Jamila, N., N. Khan, I. M. Hwang, M. Saba, F. Khan, F. Amin, S.N. Khan, A. Atlas, F. Javed, A. Minhaz and F. Ullah. 2020a. Characterization of natural gums via elemental and chemometric analyses, synthesis of silver nanoparticles, and biological and catalytic applications. *Int. J. Biol. Macromol.*, 147: 853-866.
- Jamila, N., N. Khan, A. Bibi, A. Haider, S.N. Khan, A. Atlas, U. Nishan, A. Minhaz, F. Javed and A. Bibi. 2020b. *Piper longum* catkin extract mediated synthesis of Ag, Cu, and Ni nanoparticles and their applications as biological and environmental remediation agents. *Arab. J. Chem.*, 13: 6425-6436.
- Jana, J., M. Ganguly and T. Pal. 2016. Enlightening surface plasmon resonance effect of metal nanoparticles for practical spectroscopic application. *RSC Adv.*, 6: 86174-86211.
- Johnson, A. and P. Uwa. 2019. Eco-friendly synthesis of iron nanoparticles using *Uvaria chamae*: Characterization and biological activity. *Inorg. Nano-Met. Chem.*, 49: 431-442.
- Khan, I., K. Saed and I. Khan. 2019. Nanoparticles: Properties, applications and toxicities. *Arab. J. Chem.*, 12: 908-931.
- Mirzaei, H. and M. Darroudi. 2017. Zinc oxide nanoparticles: Biological synthesis and biomedical applications. *Ceram. Int.*, 43: 907-914.
- Nithya, P. and M. Sundrarajan. 2020. Ionic liquid functionalized biogenic synthesis of AgAu bimetal doped CeO₂ nanoparticles from *Justicia adhatoda* for pharmaceutical applications: Antibacterial and anti-cancer activities. *J. Photochem. Photobiol.*, 202: 111706.
- Peng, J., G. Liu, D. Yuan, S. Feng and T. Zhou. 2017. A flow-batch manipulated Ag NPs based SPR sensor for colorimetric detection of copper ions (Cu²⁺) in water samples. *Talanta*, 167: 310-316.
- Priyadarshini, E. and N. Pradhan. 2017. Gold nanoparticles as efficient sensors in colorimetric detection of toxic metal ions: a review. *Sensor Actuat. B*, 238: 888-902.
- Puja, P. and P. Kumar. 2019. A perspective on biogenic synthesis of platinum nanoparticles and their biomedical applications. *Spectrochim. Acta A*, 211: 94-99.

- Raghunath, A. and E. Perumal. 2017. Metal oxide nanoparticles as antimicrobial agents: a promise for the future. *Int. J. Antimicrob. Agents*, 49: 137-152.
- Samuel, M.S., S. Jose, E. Selvarajan, T. Mathimani and A. Pugazhendhi. 2020. Biosynthesized silver nanoparticles using *Bacillus amyloliquefaciens*; Application for cytotoxicity effect on A549 cell line and photocatalytic degradation of p-nitrophenol. *J. Photochem. Photobiol.*, 202: 111642.
- Saratale, R.G., G.D. Saratale, H.S. Shin, J.M. Jacob, A. Pugazhendhi, M. Bhaisare and G. Kumar. 2018. New insights on the green synthesis of metallic nanoparticles using plant and waste biomaterials: current knowledge, their agricultural and environmental applications. *Environ. Sci. Pollut. Res.*, 25: 10164-10183.
- Singh, P., Y.J. Kim, D. Zhang and D.C. Yang. 2016. Biological synthesis of nanoparticles from plants and microorganisms. *Trends Biotechnol.*, 34: 588-599.
- Trim, A.R. 1951. Occurrence of Asperuloside in *Daphniphyllum macropodum* (Euphorbiaceæ) and a closely related Glucoside in *Monotropa hypopitys* Walt.(Pyrolaceæ). *Nature*, 167: 485-485.
- Trofast, J. 1978. Chloromycorrhizinol A, a furochroman from an isolate of the roots of *Monotropa hypopitys*. *Phytochem.*, 17: 1359-1361.
- Wu, Y. and L. Kong. 2020. Advance on toxicity of metal nickel nanoparticles. *Environ. Geochem. Health*, 1-10.

(Received for publication 2 April 2020)